Volume 54
Number 12
28 March 2025
Pages 4775-5194

# Dalton Transactions

An international journal of inorganic chemistry

rsc.li/dalton


ISSN 1477-9226

ROYAL SOCIETY OF CHEMISTRY

**FRONTIER**
Yuji Mikata
Bisquinoline-based fluorescent cadmium sensors

Dalton Transactions

ROYAL SOCIETY OF CHEMISTRY

FRONTIER

View Article Online
View Journal | View Issue





Cite this: *Dalton Trans.*, 2025, **54**, 4848

# Bisquinoline-based fluorescent cadmium sensors

Yuji Mikata [a,b,c,d]

Received 3rd October 2024,
Accepted 14th December 2024

DOI: 10.1039/d4dt02788d

rsc.li/dalton

Rational molecular design afforded fluorescent $Cd^{2+}$ sensors based on bisquinoline derivatives. Introduction of three methoxy groups at the 5,6,7-positions of the quinoline rings of BQDMEN (*N*,*N*′-bis(2-quinolylmethyl)-*N*,*N*′-dimethylethylenediamine) resulted in the reversal of metal ion selectivity in fluorescence enhancement from zinc to cadmium. Introduction of bulky alkyl groups and an *N*,*N*-bis(2-quinolylmethyl)amine structure, as well as replacement of one of the two tertiary amine binding sites with an oxygen atom and the use of a 1,2-phenylene backbone significantly improved the $Cd^{2+}$ specificity. The fluorescent cadmium ion selectivity could be explained by the differential binding with $Cd^{2+}$ and $Zn^{2+}$, and the formation of a bis(μ-chloro) dinuclear cadmium complex in contrast to the mononuclear zinc complex.

## 1. Introduction

Detection and quantification of toxic heavy metal ions are currently important objectives in regulation of environmental pollutants. Fluorescence sensing provides high selectivity and sensitivity toward targeted metal ions *via* a rapid analytical protocol using relatively inexpensive equipment. One of the most important issues in the detection of toxic metal ions is discrimination of $Cd^{2+}$ from naturally abundant $Zn^{2+}$, both of which are group 12 elements in the periodic table and exhibit only a 21 pm difference in their ionic radii. Since recent human activities in industry increase the exposure of cadmium to air, water and soil, continuous development of fluorescent probes for strict detection of cadmium, especially in environmental water, is in high demand. Many research groups have been investigating quinoline-based molecules for this purpose considering that the long coordination distances and softness of the quinoline nitrogen atom in comparison with conventional pyridine ligands would be suitable for selective binding with $Cd^{2+}$.[1–10] In this Frontier article, several modifications of the molecular structure of BQDMEN (*N*,*N*′-bis(2-quinolylmethyl)-*N*,*N*′-dimethylethylenediamine (**1**), Fig. 1)[11] for better $Cd^{2+}$-selectivity in the fluorescence response are discussed (Table 1). A preceding Frontier article by the present author, dealing with a related hexadentate tetrakisquinoline ligand TQEN (*N*,*N*,*N*′,*N*′-tetrakis(2-quinolylmethyl)ethylenediamine, Fig. 1), contains other examples for fluorescence sensing of $Zn^{2+}$, $Cd^{2+}$, $Hg^{2+}$ and phosphate species.[12]

## 2. Polymethoxy substitution on the quinoline ring

The BQDMEN **1** has been reported as a tetranitrogen ligand supporting mononuclear and dinuclear metal complexes including $Fe^{2+}$, $Co^{2+}$, $Ni^{2+}$, $Pd^{2+}$, $Cu^{2+/+}$, $Ru^{2+}$, $Cr^{0}$ and $Mn^{3+/2+}$ centres.[13–20] We utilized this skeleton for fluorescent $Zn^{2+}$ sensors and improved the fluorescence quantum yield by introducing a methoxy group to the quinoline rings.[11] The fluorescence turn-on mechanism includes the inhibition of photo-induced electron transfer (PeT) and chelation enhanced fluorescence (CHEF).[21–23] Thus-obtained 6-MeOBQDMEN (**2**) (Fig. 1) exhibits sufficient fluorescence intensity and $Zn^{2+}$ selectivity ($\phi_{Zn}$ = 0.28 and $I_{Zn}/I_{Cd}$ = 2.2 in DMF–$H_2O$ (1 : 1)†) for intracellular study. On the other hand, the unsubstituted BQDMEN **1** exhibits dim fluorescence ($\phi_{Zn}$ = 0.017) but slightly higher $Zn^{2+}$ selectivity ($I_{Zn}/I_{Cd}$ = 3.9) than **2**. Although we have known that further methoxy substitution does not improve the quantum yield from our study on TQEN derivatives,[24] we expected that the fluorescence metal ion selectivity could shift (or even reverse) to the $Cd^{2+}$ side. This estimation is indeed true, in which TriMeOBQDMEN **3** (Fig. 1) exhibits $Cd^{2+}$ selectivity ($I_{Zn}/I_{Cd}$ = 0.22) with similar fluorescence quantum yield ($\phi_{Cd}$ = 0.29) to the $Zn^{2+}$ complex with **2** (Table 1).[25] Interestingly, the extension of the carbon chain in the mole-

[a]*Laboratory for Molecular & Functional Design, Department of Engineering, Nara Women's University, Nara 630-8506, Japan. E-mail: mikata@cc.nara-wu.ac.jp; Fax: +81-742-20-3095; Tel: +81-742-20-3095https://eng.nara-wu.ac.jp/mikata/*
[b]*Cooperative Major in Human Centered Engineering, Nara Women's University, Nara 630-8506, Japan*
[c]*Department of Chemistry, Biology, and Environmental Science, Faculty of Science, Nara Women's University, Nara 630-8506, Japan*
[d]*KYOUSEI Science Center, Nara Women's University, Nara 630-8506, Japan*

† The DMF-$H_2O$ (1 : 1) was used as a solvent for spectroscopic measurements in the first half (Sections 2 and 3) of this article.

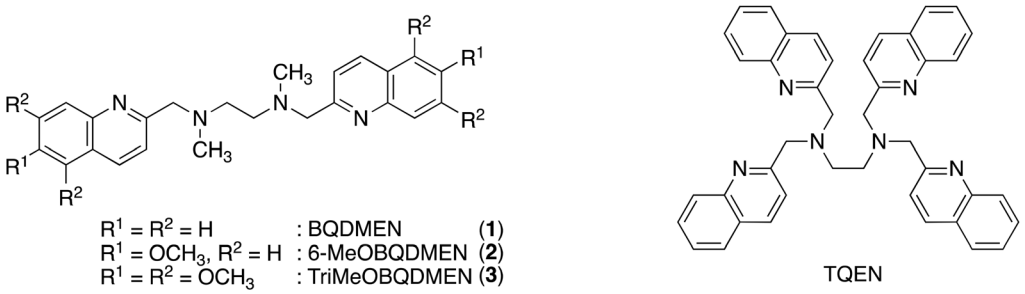


**Fig. 1** Structure of BQDMEN derivatives **1**–**3** and TQEN.

**Table 1** Fluorescence properties of $Cd^{2+}$ probes

| | $\lambda_{ex}$ (nm) | $\lambda_{em}$ (nm) | $I_{Cd}/I_0$ (eq.) | $I_{Zn}/I_{Cd}$ (eq.) | $K_d$ (metal ion) (M) | $\phi_{Cd}$ | Ref. |
|---|---|---|---|---|---|---|---|
| TriMeOBQDMEN (**3**)[a] | 339 | 472 | 15 (1) | 0.22 (1) | $\sim10^{-8}$ (Cd)<br>$\sim10^{-7}$ (Zn) | 0.29 | 25 |
| **3**[b] | 335 | 458 | 25 (3) | 0.24 (3) | $3\times10^{-7}$ (Cd)<br>$3\times10^{-6}$ (Zn) | — | 29 |
| TriMeOBQDIEN (**5**)[a] | 339 | 459 | 23 (20) | 0.04 (20) | $4\times10^{-6}$ (Cd)<br>$5\times10^{-5}$ (Zn) | 0.37 | 26 |
| TriMeOBQDBEN (**6**)[a] | 337 | 459 | 27 (3) | 0.20 (3) | $\sim10^{-7}$ (Cd)<br>$8\times10^{-6}$ (Zn) | 0.33 | 26 |
| TriMeOBQDMPHEN (**9**)[b] | 341 | 467 | 51 (1) | 0.26 (1) | $8\times10^{-7}$ (Cd)<br>$6\times10^{-6}$ (Zn) | 0.43 | 27 |
| TriMeOBQDIPHEN (**10**)[b] | 343 | 480 | 427 (40) | 0.05 (40) | $1\times10^{-3}$ (Cd)<br>$4\times10^{-2}$ (Zn) | — | 27 |
| TriMeO-*N*,*O*-BQMAE (**11**)[b] | 338 | 470 | 10 (3) | 0.34 (3) | $1\times10^{-5}$ (Cd)<br>$8\times10^{-5}$ (Cd) | 0.28 | 29 |
| TriMeO-*N*,*N*-BQMAE (**12**)[b] | 340 | 465 | 12 (3) | 0.26 (3) | $\sim10^{-7}$ (Cd)<br>$2\times10^{-5}$ (Zn) | 0.23 | 29 |
| TriMeOBQMOA (**14**)[b] | 341 | 464 | 90 (5) | 0.02 (5) | $1\times10^{-5}$ (Cd) | 0.18 | 30 |

[a] In DMF-$H_2O$ (1 : 1). [b] In DMF-HEPES buffer (1 : 1).

cular skeleton from ethylenediamine to propanediamine also shifted the fluorescence response toward the $Cd^{2+}$ side.

The fluorescence titration revealed that TriMeOBQDMEN (**3**) binds an equimolar amount of metal ions. The $Cd^{2+}$ complex with **3** exhibits significantly long fluorescence lifetime ($\tau$ = ~30 ns) in comparison with the $Zn^{2+}$ complex (~20 ns), indicating the different complex structure and/or fluorescence pathway. X-ray crystallography revealed the structures of the bis(μ-chloro) dinuclear cadmium complex and mononuclear zinc complex with BQDMEN (**1**) (Fig. 2). ESI-MS also confirmed the formation of $[(\mu\text{-Cl})_2Cd_2(\mathbf{3})_2](ClO_4)^+$ species under the spectral measurement conditions. The metal binding affinity of **3** is high enough to saturate the ligand in the presence of 1 equiv. of $Cd^{2+}$ and $Zn^{2+}$ under our experimental conditions (Table 1). These observations clearly indicate that the BQDMEN ligand discriminates $Cd^{2+}$ and $Zn^{2+}$ by differential complexation, and the introduction of three methoxy groups on the quinoline rings successfully highlights the difference in the complex structure *via* fluorescence outputs. The next step would be an improvement of the insufficient $Cd^{2+}$ selectivity of **3**. Several modifications of the molecular structure were explored to selectively reduce the $Zn^{2+}$-induced fluorescence signal.

## 3. Introduction of bulky alkyl groups

Two methyl groups of TriMeOBQDMEN (**3**) attached to the aliphatic nitrogen atoms were replaced with isopropyl groups to afford TriMeOBQDIEN (*N*,*N*′-bis(5,6,7-trimethoxy-2-quinolylmethyl)-*N*,*N*′-diisopropylethylenediamine (**5**), Fig. 3).[26] This sterically hindered bisquinoline derivative exhibits weak metal binding affinity (Table 1) and shows characteristic fluorescence titration profiles responding to $Cd^{2+}$ and $Zn^{2+}$ (Fig. 4). The highly fluorescent $Cd^{2+}$ complex with **5** ($\phi_{Cd}$ = 0.37) was formed by the addition of ~5 equiv. of $Cd^{2+}$ and was stable in the excess amount of metal ions; however, the gradual addition of $Zn^{2+}$ to **5** exhibited small fluorescence enhancement around 5 equiv. of metal ions, and then, the fluorescence significantly decreased in the presence of an excess amount of zinc salt, $Zn(ClO_4)_2$. The monomethoxy derivative (**4**) (Fig. 3) also exhibits similar profiles. After careful investigations, this observation was explained by the selective decomplexation of the zinc complex by protons generated by excess $Zn(ClO_4)_2$ used in the titration experiment. $Cd(ClO_4)_2$ did not drop the pH significantly, and the use of $Zn(NO_3)_2$ or DMF-HEPES buffer (1 : 1) as a solvent did not disrupt the $Zn^{2+}$-induced fluorescence even in the presence of a large amount of metal ions. Nevertheless, the

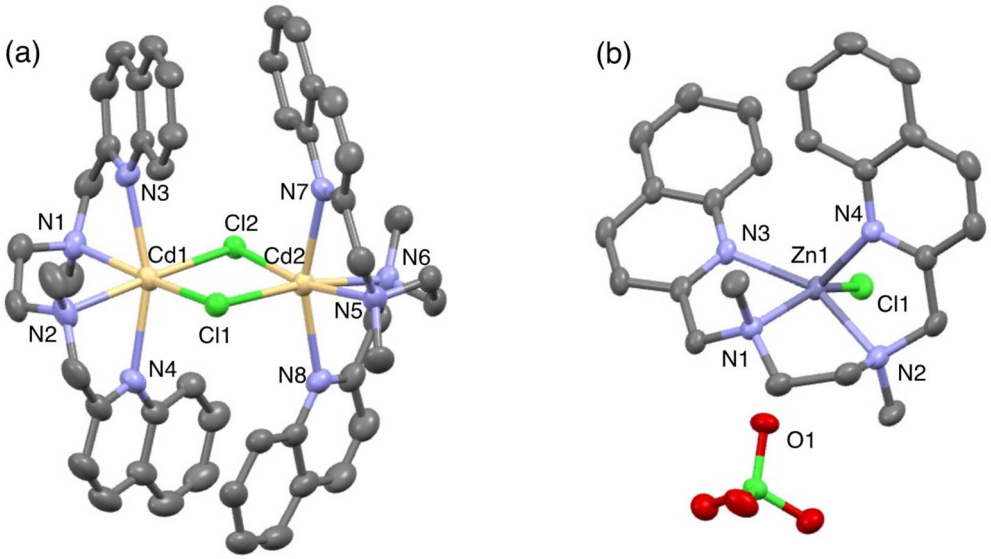


**Fig. 2** Perspective view of (a) $[(\mu\text{-Cl})_2Cd_2(\mathbf{1})_2]^{2+}$ (CSD refcode CIBKOR) and (b) $[Zn(\mathbf{1})Cl]ClO_4$ (CSD refcode CIBKUX). Reproduced from ref. 25 with permission from the Royal Society of Chemistry.

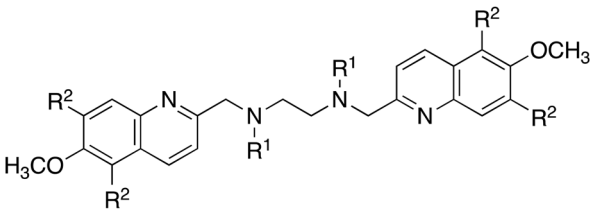


**Fig. 3** Structure of BQDMEN derivatives **4**–**7**.

excellent $Cd^{2+}$ specificity in fluorescence enhancement achieved in **5** ($I_{Zn}/I_{Cd}$ = 4% in the presence of 20 equiv. of metal ions) in DMF–$H_2O$ (1 : 1) is of significant interest.

Although X-ray crystallography employing **4** afforded only mononuclear $Cd^{2+}$ complexes, the long fluorescence lifetime ($\tau$ = ~30 ns) for the $Cd^{2+}$ complex with **5** suggested the possible formation of bis(μ-chloro) dicadmium species assembled in the excited state even in the isopropyl derivative. The corresponding benzyl (TriMeOBQDBEN (**6**)) and phenyl (TriMeOBQDPEN (**7**)) derivatives (Fig. 3) resulted in similar metal ion selectivity and fluorescence stability with **3** and an extremely poor fluorescence response with any metal ions, respectively.

## 4. Introduction of a benzene skeleton

Instead of the introduction of bulky substituents, replacement of an ethylenediamine backbone of BQDMEN (**1**) with a 1,2-

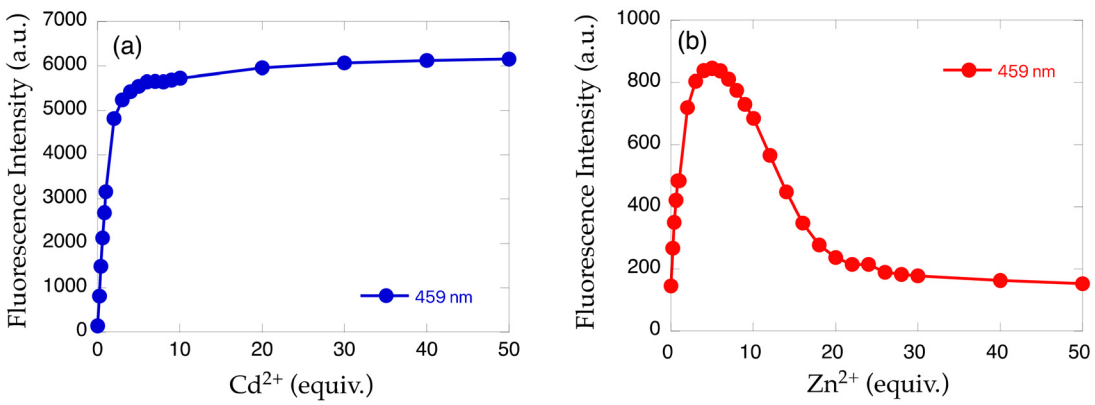


**Fig. 4** Fluorescence intensity plot of **5** with increasing amounts of (a) $Cd^{2+}$ and (b) $Zn^{2+}$.[26]

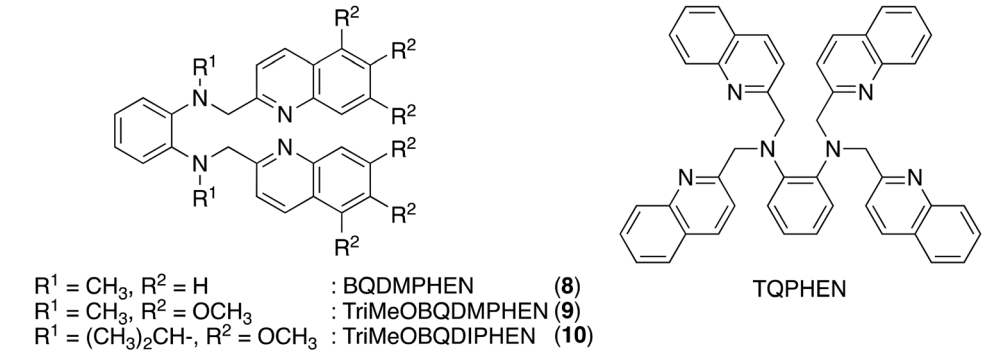


**Fig. 5** Structure of BQDMPHEN derivatives **8–10** and TQPHEN.

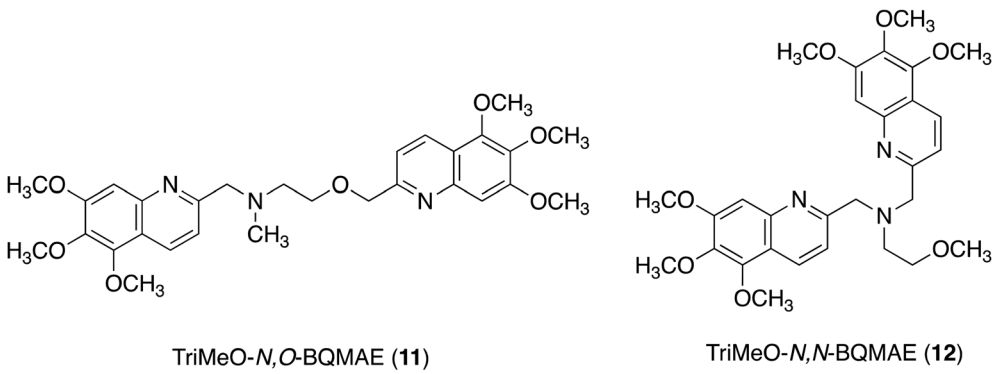


**Fig. 6** Structure of BQMAE derivatives **11** and **12**.

phenylenediamine also reduces metal binding affinity because the anilinic nitrogen atoms of BQDMPHEN (*N*,*N*′-bis(2-quinolylmethyl)-*N*,*N*′-dimethyl-1,2-phenylenediamine (**8**), Fig. 5) have weaker basicity than the aliphatic nitrogen binding site of **1**.[27] This approach has been successful for the TQEN-based tetrakisquinoline compound, TQPHEN (*N*,*N*,*N*′,*N*′-tetrakis(2-quinolylmethyl)-1,2-phenylenediamine, Fig. 5), which scarcely binds to $Zn^{2+}$ under the spectral measurement conditions and therefore exhibits $Cd^{2+}$-specific fluorescence enhancement.[28] Upon addition of metal ions in DMF-HEPES buffer (1 : 1),‡ the ligand **8** exhibited similar fluorescence enhancement with $Cd^{2+}$ and $Zn^{2+}$ ($I_{Zn}/I_{Cd}$ = 0.90 in the presence of 1 equiv. of metal ion), but apparent $Cd^{2+}$ selectivity ($I_{Zn}/I_{Cd}$ = 0.26 in the presence of 1 equiv. of metal ions) was achieved in the trimethoxy derivative (TriMeOBQDMPHEN (**9**), Fig. 5). The insufficient metal ion selectivity was further improved by introducing isopropyl groups as discussed above, affording high fluorescent $Cd^{2+}$ specificity in TriMeOBQDIPHEN (**10**) ($I_{Zn}/I_{Cd}$ = 0.05 in the presence of 40 equiv. of metal ions) (Fig. 5).

‡The DMF-HEPES buffer (1 : 1, 50 mM HEPES, 0.1 M KCl, pH = 7.5) was used as a solvent for spectroscopic measurements in the second half (Sections 4–6) of this article, considering the pH change in the presence of large amount of metal salts.

Considering the extremely weak metal binding affinity of the isopropyl ligand **10** ($K_d$(Cd) = 1 × $10^{-3}$ M), the methyl counterpart **9** ($K_d$(Cd) = 8 × $10^{-7}$ M) is more suitable for practical use (Table 1). This high metal binding affinity causes diminished $Cd^{2+}/Zn^{2+}$ selectivity estimated from the ratio of binding constants ($K_d$(Zn)/$K_d$(Cd) = 8 and 32 for **9** and **10**, respectively); however, the high fluorescence quantum yield ($\phi_{Cd}$ = 0.43) and wide pH window (pH = 4–10) of **9** are worth exploring. The structures of $Cd^{2+}$ and $Zn^{2+}$ complexes with **8** are both mononuclear but, here again, the long fluorescence lifetime ($\tau$ = ~30 ns) for $Cd^{2+}$ complexes with **9** and **10** suggests the excimer-like fluorescence mechanism including quinoline–quinoline interactions in the excited state.

## 4. Replacement of a nitrogen atom with an oxygen atom

Another strategy to reduce the metal binding affinity of the tetranitrogen ligand TriMeOBQDMEN (**3**), aiming at the improvement of fluorescent $Cd^{2+}$ selectivity, is the replacement of one of the two aliphatic ethylenediamine nitrogen atoms of **3** with an oxygen atom. Thus-designed 2-aminoethanol-based N3O1 ligand, TriMeO-*N*,*O*-BQMAE (*N*,*O*-bis(5,6,7-trimethoxy-2-quinolylmethyl)-2-methylaminoethanol (**11**), Fig. 6) exhibited two

order lower metal binding affinity and slightly decreased $Cd^{2+}$ preference in fluorescence enhancement in comparison with **3** ($I_{Zn}/I_{Cd}$ = 0.34 and 0.24 for **11** and **3**, respectively, in the presence of 3 equiv. of metal ions in DMF-HEPES buffer (1 : 1)) (Table 1).[29] Interestingly, TriMeO-*N*,*N*-BQMAE (**12**) (Fig. 6), the regioisomer of **11**, in which both quinoline moieties are attached to the same aliphatic nitrogen atom of the aminoethanol skeleton, exhibits one order higher metal binding affinity than **11** and similar fluorescent $Cd^{2+}$ selectivity to **3** ($I_{Zn}/I_{Cd}$ = 0.26 for **12**). The fluorescence quantum yield of **12** ($\phi_{Cd}$ = 0.23) is slightly smaller in comparison with those of **3** (0.29) and **11** (0.28) under the same experimental conditions. This difference is also reflected by the fluorescence lifetimes, where long fluorescence lifetimes ($\tau$ = ~30 ns) with a possible intramolecular excimer emission for the $Cd^{2+}$ complex were observed only for **3** and **11**. For the *N*,*N*-isomer **12**, no difference in fluorescence lifetimes of $Zn^{2+}$ and $Cd^{2+}$ complexes was detected ($\tau$ = ~18 ns), indicating the monomer emission for both metal complexes with this ligand. The ligand structure of **12** strictly controls the metal binding affinity, possibly due to the difference in the complex structures, affording the fluorescent $Cd^{2+}$ selectivity. It is important to note that the two order difference in dissociation constants between $Cd^{2+}$ and $Zn^{2+}$ complexes was achieved in the *N*,*N*-bisquinoline structure of **12** (Table 1). The corresponding *N*,*N*-isomer for **3** has not been examined due to problems in its synthesis.

## 5. Use of a benzene skeleton with an oxygen binding site

Finally, the N3O1 ligand with a 1,2-phenylene skeleton was explored. Considering the synthetic accessibility, only the *N*,*N*-isomer was examined here. Thus-designed TriMeOBQMOA (*N*,*N*-bis(5,6,7-trimethoxy-2-quinolylmethyl)-2-methoxyaniline (**14**), Fig. 7) exhibits excellent $Cd^{2+}$ specificity in fluorescence enhancement ($I_{Zn}/I_{Cd}$ = 0.02 in the presence of 5 equiv. of metal ions) with moderate metal binding affinity ($K_d$(Cd) = 1 × $10^{-5}$ M) and fluorescence quantum yield ($\phi_{Cd}$ = 0.18) (Table 1).[30] The binding affinity of **14** with $Zn^{2+}$ is extremely weak. The LOD (limit of detection) for $Cd^{2+}$ was estimated to

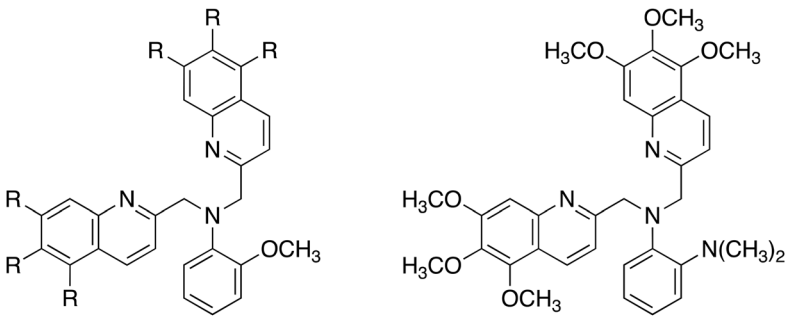


Fig. 7 Structure of BQMOA and BQDMPHEN derivatives **13**–**15**.

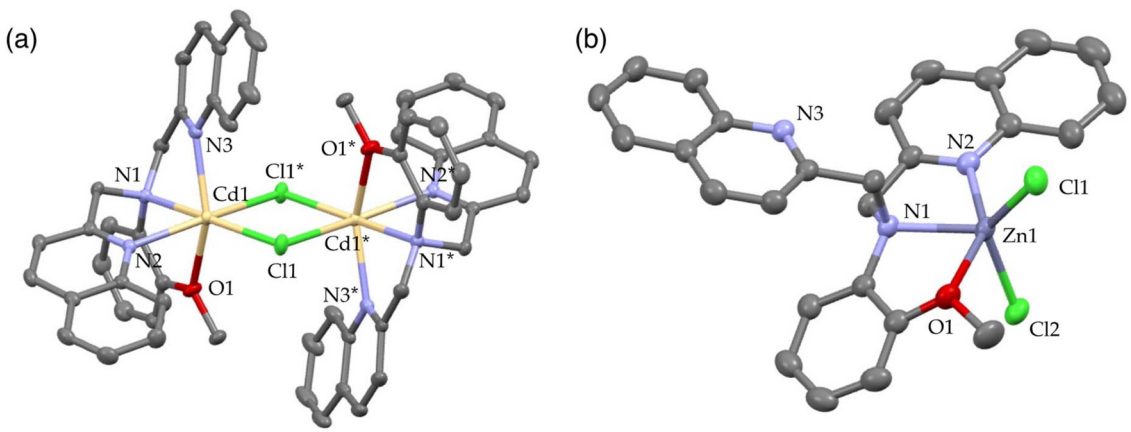


Fig. 8 Perspective view of (a) $[(\mu\text{-Cl})_2Cd_2(\mathbf{13})_2]^{2+}$ (CSD refcode YOMQOK) and (b) $[Zn(\mathbf{13})Cl_2]$ (CSD refcode YOMQUQ). Adapted from ref. 30 with permission from American Chemical Society, copyright 2024.

 

be 25 nM, which is lower than the environmental limit of water in Japan (3 ppb, 27 nM).

Both $Cd^{2+}$ and $Zn^{2+}$ complexes with BQMOA (**13**) (Fig. 7) were structurally characterized by X-ray crystallography (Fig. 8) where the bis(μ-chloro) dinuclear cadmium complex ($[(\mu\text{-}Cl)_2Cd_2(\mathbf{13})_2]^{2+}$) and mononuclear zinc complex ($[Zn(\mathbf{13})Cl_2]$) with an uncoordinated quinoline moiety were revealed. These complex structures clearly explain the reason for the short fluorescence lifetime ($\tau$ = ~13 ns) for the $Cd^{2+}$ and $Zn^{2+}$ complexes with **14** because of the lack of interquinoline stacking interaction even in the bis(μ-chloro) dicadmium complex. The fluorescent $Cd^{2+}$ specificity is a result of the extremely weak binding affinity of this ligand with $Zn^{2+}$.

The importance of chloride ions in HEPES buffer was also disclosed in this study. As shown in Fig. 9, chloride ions exclusively enhance the fluorescence intensity of **14** in the presence of $Cd^{2+}$ *via* enhanced complexation, but no such effect was observed for $Zn^{2+}$ with **14** and dimethylamino derivative

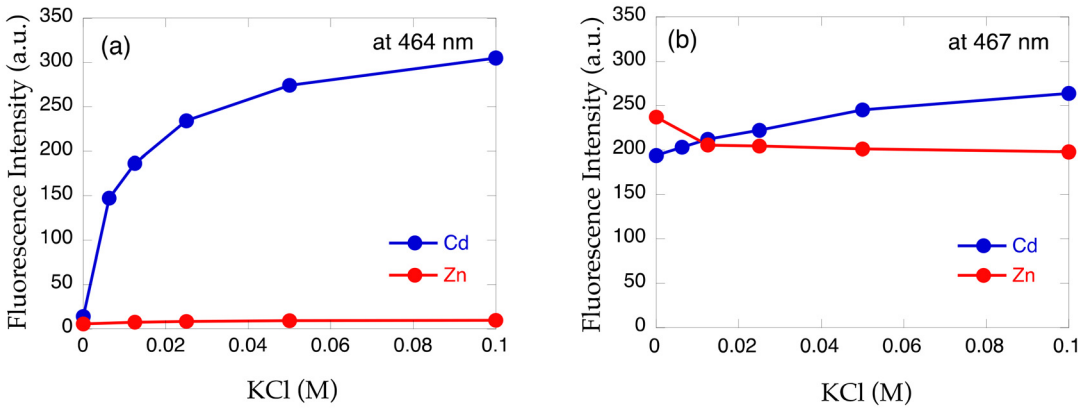


**Fig. 9** Fluorescence intensity plot of (a) **14** and (b) **15** in the presence of $Cd^{2+}$ (blue) or $Zn^{2+}$ (red) with increasing amount of KCl. Adapted from ref. 30 with permission from American Chemical Society, copyright 2024.

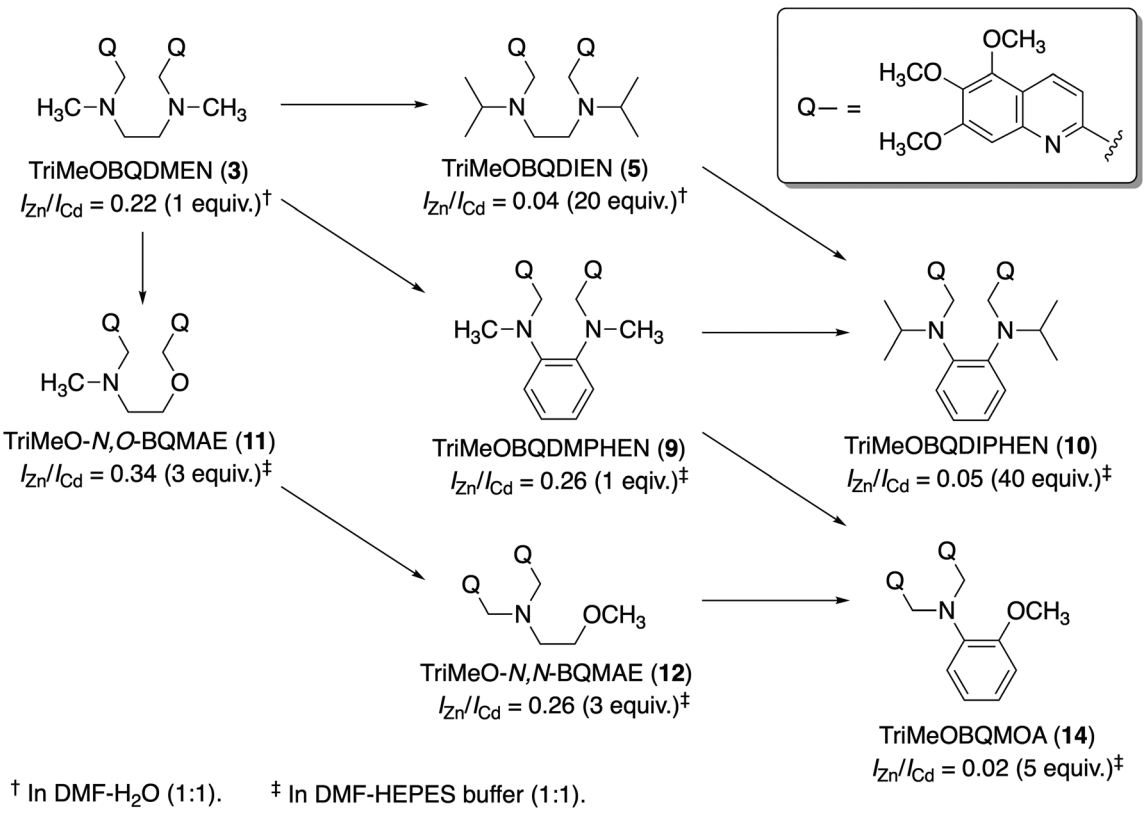


**Fig. 10** Summary of the structural modifications of $Cd^{2+}$ probes.

TriMeO-*N*,*N*-BQDMPHEN (*N*,*N*-bis(5,6,7-trimethoxy-2-quinolylmethyl)-*N*′,*N*′-dimethyl-1,2-phenylenediamine (**15**), Fig. 7) with $Cd^{2+}$ and $Zn^{2+}$. Not only the moderate metal binding affinity but also the appropriate size and coordination environment of the metal binding cavity of the methoxy derivative **14** in the presence of chloride ions are necessary for fluorescence discrimination of $Cd^{2+}$ from $Zn^{2+}$.

## 6. Conclusions

Based on the structure of BQDMEN (**1**), a set of fluorescent $Cd^{2+}$ sensors were rationally designed (Fig. 10). The extensive use of polymethoxy-substituted quinolines as a metal binding motif and chromophore provides several unique characteristics suitable for strict discrimination of $Cd^{2+}$ from $Zn^{2+}$ *via* fluorescence signals. Unprecedented fluorescence enhancement mechanisms including intramolecular excimer emission from the bis(μ-chloro) dinuclear cadmium complex were clarified by X-ray crystallography. Tiny changes in the molecular structure of the fluorescent probe largely affect the structure and stability of the resulting metal complexes, affording significant improvement in fluorescent metal ion selectivity and optical properties. In particular, the size and flexibility of the metal binding pocket with a carefully organized coordination geometry are crucial for selective accommodation of the target metal ion. This Frontier article may provide a useful dataset for future molecular design of new fluorescent sensors targeting a wide variety of metal ions.

## Data availability

No primary research results, software or code have been included and no new data were generated or analysed as part of this review.

## Conflicts of interest

There are no conflicts to declare.

## Acknowledgements

The author expresses sincere thanks to his students and collaborators for their valuable help in the exploration of BQDMEN-based ligands. This work was also supported by the JSPS KAKENHI Grant Number JP23K04808 and the Nara Women's University Intramural Grant for Project Research.

## References

1 X.-L. Tang, X.-H. Peng, W. Dou, J. Mao, J.-R. Zheng, W.-W. Qin, W.-S. Liu, J. Chang and X.-J. Yao, *Org. Lett.*, 2008, **10**, 3653–3656.
2 L. Xue, G. Li, Q. Liu, H. Wang, C. Liu, X. Ding, S. He and H. Jiang, *Inorg. Chem.*, 2011, **50**, 3680–3690.
3 M. Mameli, M. C. Aragoni, M. Arca, C. Caltagirone, F. Demartin, G. Farruggia, G. De Filippo, F. A. Devillanova, A. Garau, F. Isaia, V. Lippolis, S. Murgia, L. Prodi, A. Pintus and N. Zaccheroni, *Chem. – Eur. J.*, 2010, **16**, 919–930.
4 X. Zhou, P. Li, Z. Shi, X. Tang, C. Chen and W. Liu, *Inorg. Chem.*, 2012, **51**, 9226–9231.
5 H. Tian, B. Li, J. Zhu, H. Wang, Y. Li, J. Xu, J. Wang, W. Wang, Z. Sun, W. Liu, X. Huang, X. Yan, Q. Wang, X. Yao and Y. Tang, *Dalton Trans.*, 2012, **41**, 2060–2065.
6 Y. Li, H. Chong, X. Meng, S. Wang, M. Zhu and Q. Guo, *Dalton Trans.*, 2012, **41**, 6189–6194.
7 Y. Ma, F. Wang, S. Kambam and X. Chen, *Sens. Actuators, B*, 2013, **188**, 1116–1122.
8 X.-J. Jiang, M. Li, H.-L. Lu, L.-H. Xu, H. Xu, S.-Q. Zang, M.-S. Tang, H.-W. Hou and T. C. W. Mak, *Inorg. Chem.*, 2014, **53**, 12665–12667.
9 E. Hrishikesan, R. Manjunath and P. Kannan, *J. Solution Chem.*, 2016, **45**, 907–919.
10 D. Udhayakumari, *J. Mol. Struct.*, 2023, **1287**, 135715.
11 Y. Mikata, A. Yamashita, A. Kawamura, H. Konno, Y. Miyamoto and S. Tamotsu, *Dalton Trans.*, 2009, 3800–3806.
12 Y. Mikata, *Dalton Trans.*, 2020, **49**, 17494–17504.
13 B. Rieger, A. S. Abu-Surrah, R. Fawzi and M. Steiman, *J. Organomet. Chem.*, 1995, **497**, 73–79.
14 A. S. Abu-Surrah, U. Thewalt and B. Rieger, *J. Organomet. Chem.*, 1999, **587**, 58–66.
15 A. S. Abu-Sarrah, *Asian J. Chem.*, 2002, **14**, 1251–1256.
16 Y. Mikata, H. So, A. Yamashita, A. Kawamura, M. Mikuriya, K. Fukui, A. Ichimura and S. Yano, *Dalton Trans.*, 2007, 3330–3334.
17 L. S. Morris, M. P. Girouard, M. H. Everhart, W. E. McClain, J. A. van Paridon, R. D. Pike and C. Goh, *Inorg. Chim. Acta*, 2014, **413**, 149–159.
18 M. Saga, T. Anamushi, W. Miyahara, S. Yamazaki and K. Saito, *Anal. Sci.*, 2015, **31**, 185–189.
19 N. Singh, J. Niklas, O. Poluektov, K. M. Van Heuvelen and A. Mukherjee, *Inorg. Chim. Acta*, 2017, **455**, 221–230.
20 R. V. Ottenbacher, A. G. Medvedev, A. A. Nefedov and K. P. Bryliakov, *Inorg. Chem. Commun.*, 2023, **156**, 111282.
21 A. P. de Silva, H. Q. N. Gunaratne, T. Gunnlaugsson, A. J. M. Huxley, C. P. McCoy, J. T. Rademacher and T. E. Rice, *Chem. Rev.*, 1997, **97**, 1515–1566.
22 B. Daly, J. Ling and A. P. de Silva, *Chem. Soc. Rev.*, 2015, **44**, 4203–4211.
23 D. Escudero, *Acc. Chem. Res.*, 2016, **49**, 1816–1824.
24 Y. Mikata, M. Wakamatsu, A. Kawamura, N. Yamanaka, S. Yano, A. Odani, K. Morihiro and S. Tamotsu, *Inorg. Chem.*, 2006, **45**, 9262–9268.
25 Y. Mikata, M. Tanaka, S. Yasuda, A. Tsuruta, T. Hagiwara, H. Konno and T. Matsuo, *Dalton Trans.*, 2023, **52**, 7411–7420.
26 Y. Mikata, S. Yasuda, T. Hagiwara, H. Konno and S. Shoji, *Inorg. Chim. Acta*, 2024, **571**, 122218.

 

27 Y. Mikata, K. Kawakami, M. Nagaoka, S. Shoji, H. Konno and T. Matsuo, *Inorg. Chim. Acta*, 2024, **565**, 121968.
28 Y. Mikata, A. Kizu and H. Konno, *Dalton Trans.*, 2015, **44**, 104–109.
29 Y. Mikata, A. Tsuruta, H. Koike, S. Shoji and H. Konno, *Molecules*, 2024, **29**, 369.
30 Y. Mikata, N. Tosaka, S. Yasuda, Y. Sakurai, S. Shoji, H. Konno and T. Matsuo, *Inorg. Chem.*, 2024, **63**, 8026–8037.